

Chapter 2

Two Typical Plant Aggregates for Bio-Based Concretes

Hemp shiv (well-known) and rice husk (novel)

Many by-products of plant origin have been incorporated in mineral binders. However, it is important to distinguish plant fibers used as reinforcement in cement composite materials from plant-derived aggregates used for the manufacturing of lightweight insulating concretes (bio-based concretes). Those can be defined as the association of a high volume fraction of crop residues with a mineral binder [1]. This book does not deal with load-bearing concretes with very small amounts of aggregates or reinforcing fibers.

Most of the plant aggregates are derived from stems (hemp, flax, sunflower), straws (sorghum or miscanthus) and trunks (woodchips).

After grinding, the woody part of hemp stems gives rise to hemp shiv, a well-known aggregate associated with a lime-based binder to design Lime and Hemp Concrete (LHC). In order to diversify crop by-products, a novel kind of aggregate is explored. It corresponds to rice husk, the protective shell of rice grains. Since rice husk particles come from a totally different part of the plant, their characteristics will be presented and compared to those of hemp shives.

2.1 Source and Transformation Processes

2.1.1 Hemp Shiv

Hemp (*Cannabis Sativa*) is an annual plant whose height is from 1–3 m (Fig. 2.1a). This species is dedicated to the cultivation of industrial hemp in Central Asia and Europe. Hemp is grown as a break crop and harvested after 4 months of maturity [2, 3]. Thereafter, stems are cut and left on the field for a few weeks (retting). When the moisture content of stems is around 15%, those are harvested and taken to the defibering process to separate the woody part from the fibers (Fig. 2.1b).

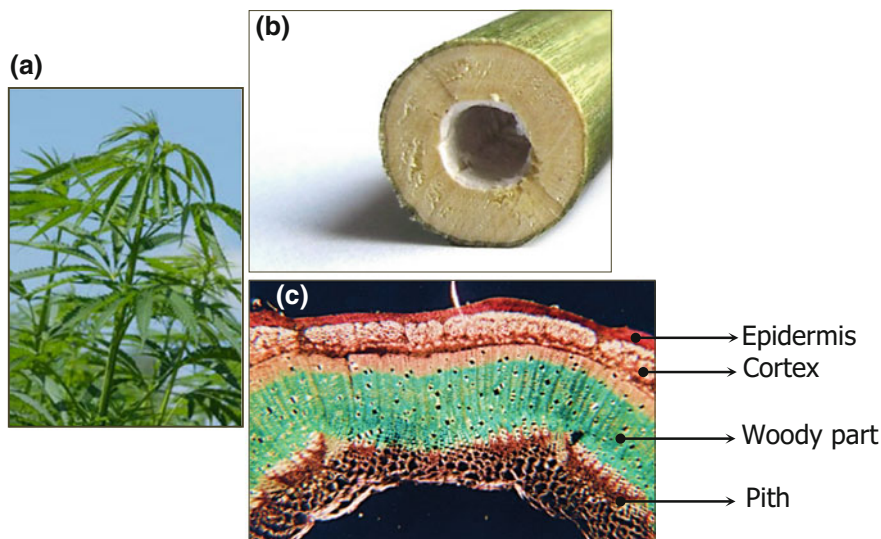


Fig. 2.1 **a** Hemp plant **b** Hemp stem **c** Micrograph of a cross-sectional view of a hemp stem colored with *green Carmino of Mirande* [3] (color figure online)

A micrograph of a cross-sectional view of a hemp stem colored with *green Carmino of Mirande* is reported in Fig. 2.1c. It makes it possible to describe cellulose-rich areas (in red) from those which are strongly lignified (in green) [3]:

- The epidermis consists of cells with cellulosic walls.
- The cortex contains the phloem fibers grouped into bundles.
- The woody part (from which the hemp shiv mainly comes) consists of parenchymal cells and xylem vessels.
- The cellulosic pith corresponds to the medullary parenchyma.

Plant tissues are rich in cellulosic compounds except the woody part for which the lignin content is clearly higher than in other areas (Fig. 2.1c). The woody part accounts for 50 wt% of the dry stem. As a result, the production yield of hemp shives is 3–3.5 T/ha (tons per hectare) or approximately 35,000 tons per year in France [4].

In France, the use of hemp shiv as lightweight aggregate for the manufacturing of LHC was initiated in the early 1990s.

After grinding, hemp shiv is in the form of chips whose morphological properties will be addressed. The shiv presented in this book is in compliance with the French professional rules for the construction of hemp concrete structures [5, 6] (Fig. 2.2).

The plant-based concretes studied by the authors will be manufactured with a shiv which either comes from FRD[®] (Troyes, France) or Technichanvre[®] (Riec-sur-Bélon, France).

Fig. 2.2 Commercial hemp shiv



2.1.2 Rice Husk

According to figures from the International Grains Council (IGC) [7], rice is the first cereal in the world for human food before wheat and corn. This is due to the non-food use of rice which remains marginal if compared to wheat. Furthermore, rice is locally grown in the South of France. It is particularly important to favor local resources for the design of bio-based concretes as it is an opportunity to develop eco-friendly materials by minimizing the impact of transport. In France, rice fields are located in the Camargue area. The production of rough rice in France is about 80,000 tons per year (according to a source in 2013) [8].

Rice harvest firstly consists in separating grains from straws and removing impurities (insects, minerals and residues). Thereafter, rice grains undergo a drying process before the husking where the outer covering is removed from the grain. Rice husks are defined by two interlocking halves with a boat-like shape (lemma and palea are botanical terms) for each rice grain [9]. When any other transformation process occurs, rice husk is qualified as natural. By contrast, some varieties are parboiled. In the latter case, rice grains are soaked and exposed to water vapor before the husking.

Rice husk (*Oryza Sativa*) can be considered as an agro-industrial by-product coming from the rice hulling. This crop residue represents about 20 wt% of the whole rough rice (i.e. paddy rice) harvested on the spikelets [10]. Hence, rice farming produces nearly 15,000 tons of rice husks per year in France. Currently, the use of rice husk is highly limited, this latter being regarded as a waste material often buried in the ground or used as a fuel. Indeed, rice husk can be consumed for electricity generation because of its high calorific value. However, the incineration process is dangerous to human health and to the environment. Therefore, rice husk causes critical problems in rice growing areas since significant volumes are generated and not used in a beneficial way [11]. In the building sector, the use of rice husk ash as pozzolanic filler in cementitious binders was widely referenced [10, 12–16].

Fig. 2.3 Natural rice husk

Rice husk is characterized by a lower content of organic matter compared to other lignocellulosic by-products since it contains about 20% of amorphous silica [12, 17]. Consequently, when rice husk is burnt beyond 500 °C, the organic matter disappears and gives way to a SiO₂-rich nanometric ash with interesting pozzolanic properties [12, 16].

The use of whole rice husk as plant aggregate to design bio-based concretes is therefore totally novel. In this context, rice husks present many substantial advantages. They do not flame or smolder easily because of their particular silica-cellulose structural arrangement [18]. Moreover, given that husks do not biodegrade or burn easily, they are sometimes free-of-charge. Another asset is their availability throughout the year because most farms store rice and process it on a daily basis. Furthermore, it should be noted that hemp shives result from an industrial grinding process whereas rice husks can be used as they stand, requiring no shredding.

Natural rice husks presented here have not undergone any parboiling process and come from Biosud (Arles, France) (Fig. 2.3).

2.2 Chemical Composition

Lignocellulosic plants can be described at the cell wall scale. Cellulose and lignin represent about 70% of the plant biomass [1]. The structure of the cell wall is illustrated in Fig. 2.4 [19, 20].

The middle lamella (ML in Fig. 2.4a) is rich in pectin and acts as an adhesive between the cells. The primary cell wall (P) consists of cellulose microfibrils which lie parallel to each other. These chains of crystallized cellulose are embedded in an amorphous matrix of hemicelluloses (Fig. 2.4b). The secondary cell wall is divided

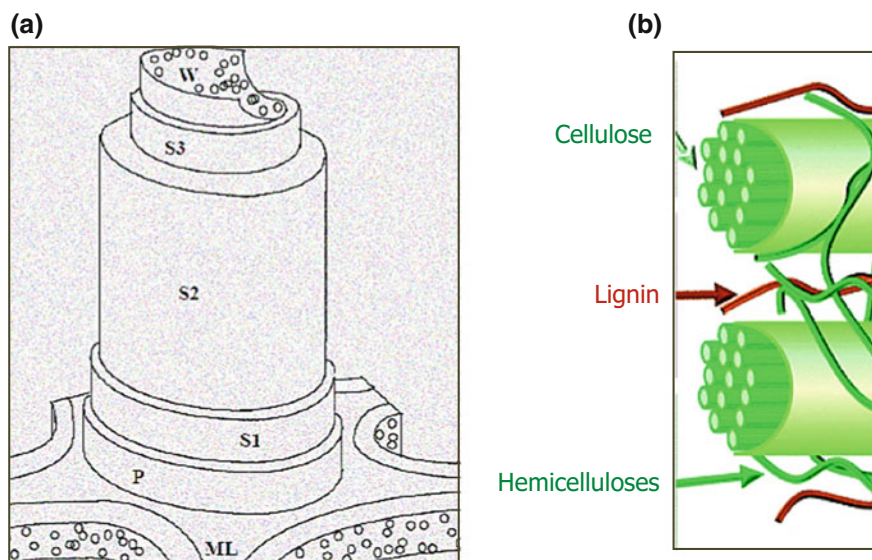


Fig. 2.4 **a** Cell wall of lignocellulosic plants **b** Arrangement of chemical components in the cell wall [20]

into three different layers (S₁, S₂ and S₃). It contains the same components than the primary cell wall but it is characterized by a higher lignin content [1, 3, 19, 20].

Plant-derived by-products have the same components (cellulose, hemicelluloses, lignin, pectins, waxes) but in variable proportions.

- Cellulose is a linear polysaccharide polymer with many glucose units. Owing to its strong inter and intra-bondings, mainly hydrogen bonds, cellulose is insoluble in most solvents. However, it is highly hydrophilic [1, 3, 19].
- Hemicelluloses are short-chained polysaccharides with an amorphous structure. Contrary to cellulose which contains only one sugar, hemicelluloses consist of several sugar units (glucose, galactose, mannose, arabinose, xylose, rhamnose) and uronic acids. Hemicelluloses are soluble in water and easily extracted from cell walls thanks to alkaline solutions. They are also hydrophilic [1, 3, 19].
- Lignin is a complex polymer with aliphatic and aromatic chains. The lignin content is especially high in the woody part of stems (xylem). Lignin provides stiffness and impermeability. It is effectively very hydrophobic (contrary to holocellulose) [1, 3].
- Pectins are acidic polysaccharides present in the middle lamella. Their carboxyl groups have a great capacity to exchange Ca²⁺ [3].
- Waxes consist of water-insoluble alcohols and acids. They can be extracted with organic solutions and are hydrophobic.

The chemical composition of plant aggregates coming from some studies is reported in Table 2.1.

Table 2.1 Chemical composition of plant aggregates (in weight percentages)

(%)	Hemp shiv [21, 22]	Rice husk [23, 24]
Cellulose	46–48	25–35
Hemicelluloses	12–21	18–21
Lignin	22–28	26–31
Extractives ^a	11–16	2–5
Silica ash	–	15–25

^aWaxes, fats, pectins and sugars extracted by different aqueous solutions

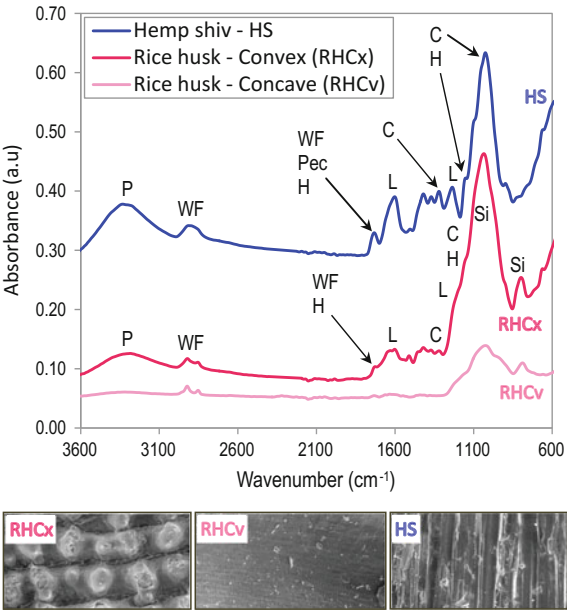
As expected, rice husk is lower than hemp shiv in total organic matter owing to its silica ash content which is particularly high for a plant particle. The lignin content is the same in both cases but rice husk is actually lower in total carbohydrates since it contains less cellulose and extractives.

The chemical composition of plant particles depends on the plant variety but also the cultivation area, the soil conditions or even the plant maturity.

FTIR spectra (i.e. Fourier Transformed Infrared Spectroscopy) of plant particles are reported in Fig. 2.5.

Surfaces of particles (convex and concave for rice husk) are analyzed. The presence of amorphous polysaccharides such as hemicelluloses, pectins, waxes but also natural fats is highlighted by the presence of the band around 3300 cm⁻¹ and peaks around 2900 and 1730 cm⁻¹. Lignin-associated absorbances are visible at 1600 and 1240 cm⁻¹ as a peak for hemp shiv and a broad shoulder for rice husk. The peak at 1320 cm⁻¹ corresponds to cellulose. For hemp shiv, the peak at

Fig. 2.5 FTIR spectra of plant particles.
P polysaccharides, *WF* waxes and fats, *Pec* pectins, *H* hemicelluloses, *L* lignin, *C* cellulose, *Si* Silica [25]



1030 cm^{-1} is associated to both hemicelluloses and cellulose. However, for rice husk, the broad band in the range $900\text{--}1200\text{ cm}^{-1}$ is attributed to cellulosic compounds but also to silica. It was shown in Table 2.1 that rice husk contains less cellulose than hemp shiv but a significant quantity of silica on its surface. The peak corresponding to stretching vibrations of Si–C bonds at 800 cm^{-1} confirms the presence of silica for rice husk.

2.3 Physical and Morphological Properties

2.3.1 Microstructure

The cross-sectional view of a single particle by scanning electron microscopy (SEM) is reported in Fig. 2.6.

Figure 2.6b highlights the huge porosity of hemp shiv which is characterized by a honeycombed structure with lots of vessels whose diameter is more than $10\text{ }\mu\text{m}$. The latter can be up to $60\text{ }\mu\text{m}$ [26]. The vessels are oriented longitudinally in the particle. The thickness of the walls between them is no more than $1\text{ }\mu\text{m}$. The internal structure of a rice husk is different (Fig. 2.6a). Some little vessels can be observed but the solid phase appears to be in a majority proportion. Jauberthie et al. [12] and Park et al. [27] described the detailed microstructure of rice husk and the distribution of amorphous silica in the particle. Different SEM pictures are reported in Fig. 2.7.

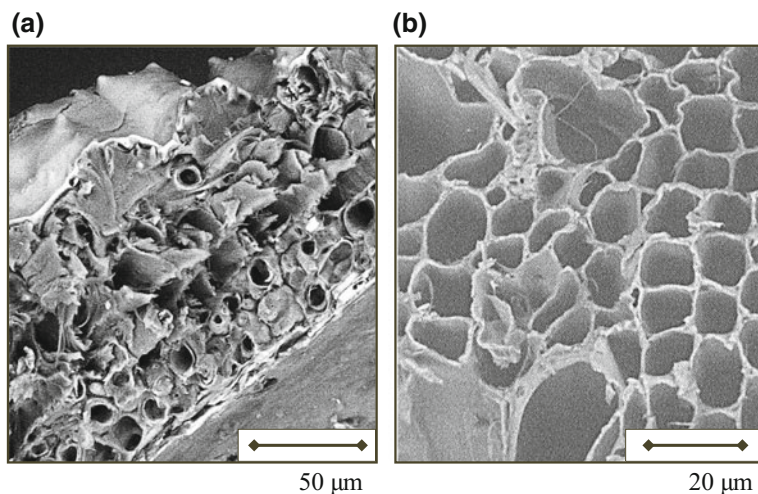


Fig. 2.6 SEM pictures of rice husk (a) and hemp shiv (b)

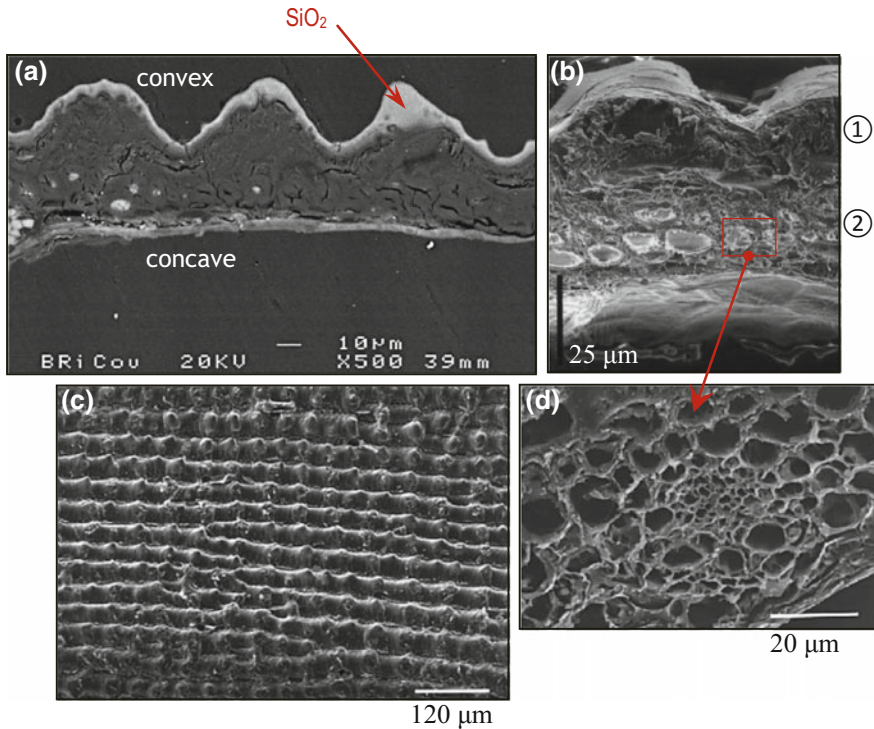


Fig. 2.7 **a** Silica distribution on a cross-sectional view of rice husk **b** Cross-sectional view of rice husk from the external epidermis to the internal epidermis **c** Morphology of the external epidermis of rice husk **d** Cross section of vascular bundles [12, 27]

The external surface (convex face) of the husk is characterized by a peculiar morphology. The epidermal cells are arranged in furrows and linear ridges with dome-shaped protrusions [27] (Fig. 2.7c). This external epidermis is rich in amorphous silica as shown in Fig. 2.7a. The layers of fibers underlying the outer epidermis are highly thick-walled according to Park et al. [27]. This area is strongly lignified and lowly porous (Fig. 2.7b, area n°1). The inner part of rice husk tissue shows a well-defined area with vascular bundles (Fig. 2.7b, area n°2). These are longitudinal vessels of phloem and xylem as they can be observed within the hemp particle. This area is significantly more porous than that consisted of the thick-walled epidermis and fibers. This is attested by Fig. 2.7d. From the external epidermis (convex) to the internal epidermis (concave), tissue organization consists of outer epidermis, layers of fibers, vascular bundles, parenchyma cells and inner epidermis. The area close to the inner epidermal cells is poorly lignified and thin-walled. The inner epidermis (concave face) is smoother than the outer one and it contains less silica. The silica content in internal tissues is negligible [12].

2.3.2 Densities and Porosities

The total porosity of bulk aggregates is related to the intergranular porosity and to the porosity within the particles. The knowledge of the bulk density, the apparent density of a particle (including the internal voids as presented in Fig. 2.8) and the true density of the solid phase make it possible to calculate the different porosities. These physical characteristics are all reported in Table 2.2.

Fig. 2.8 Schematic representation of a plant particle and its porosity

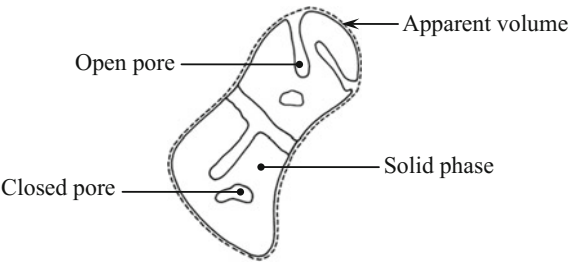


Table 2.2 Densities and porosities of plant aggregates

Notation ^a	Method	Hemp shiv	Rice husk
		g cm ⁻³	
ρ_B	–	0.1	0.09
ρ_A	Estimated ^b	0.24	0.53
	Paraffin method [28]	–	0.65
	Stem section ^c [2]	0.26	–
ρ_T	Helium pycnometry ^d	–	1.48
	Air pycnometry [28]	–	1.42
	C ₇ H ₈ pycnometry ^e [2]	1.47	–
		%	
η_O	$1 - \rho_A / \rho_T$	82–84	54–64
η_I	$1 - \rho_B / \rho_A$	58–62	83–86
η_T	$1 - \rho_B / \rho_T$	93	94

^aNomenclature

ρ_B —Bulk density

ρ_A —Apparent density (particle)

ρ_T —True density (solid phase)

η_O —Open porosity in the particle

η_I —Intergranular porosity

η_T —Total porosity in the bulk

^bParticle density was calculated from the known pycnometric true density (ρ_T) and the water absorption capacity of particles after saturation (W_S) with this expression: $\eta_O = (W_S \times \rho_T) / [\rho_W + (W_S \times \rho_T)]$ where ρ_W is the density of water and W_S was taken as 120 wt% for rice husk [29] and 370 wt% for hemp shiv [1]

^cMeasurement on the basis of image analysis of a straight section of hemp stem

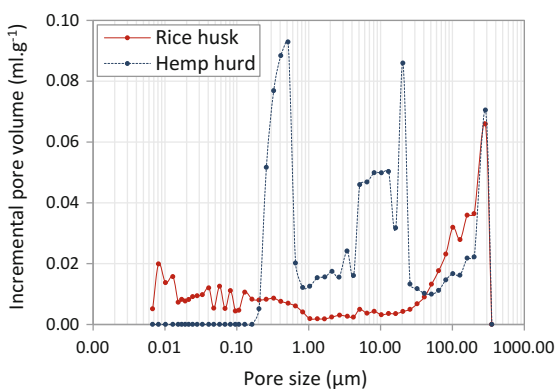
^dMeasured by the authors

^eToluene pycnometry

Table 2.2 shows that bulk density is about 0.1 g cm^{-3} for the two kinds of aggregates. Apparent and true densities are more difficult to measure. Some studies in literature report an underestimated value of the true density of rice husk [11, 29, 30] measured by the water displacement method. The latter has proved to be not accurate for plant particles as air is trapped in the pores [28]. The true density of rice husk is 1.48 g cm^{-3} according to Helium pycnometry. This result is very close to that reported in the work of Kaupp [28] in which air pycnometry has been used (1.42 g cm^{-3}). Moreover, the true density of rice husk is equivalent to that of hemp shiv (Table 2.2). This value is itself close to the pycnometric density of wood which is equal to 1.54 g cm^{-3} according to Rowell [31]. Apparent density can be calculated with the true density and the porosity within the particle. The rate of water absorption has to be known to access this porosity [1, 29]. It is interesting to see that the estimated apparent density using this method is relatively close to that measured by the paraffin method by Kaupp [28] (rice husk) or directly on the stem by Nguyen [2] (hemp). Either way, the apparent density of rice husk is more than twice that of hemp shiv (Table 2.2). This results in a lower internal porosity but a higher intergranular porosity for rice husk. The total porosity is finally the same for bulk aggregates (Table 2.2). It shows the strong propensity of these particles to provide a very good capacity for thermal insulation. It should be noted that the open porosity within hemp particles is very high and interconnected [32]. As regards rice husk, some authors [33, 34] refer to a certain amount of closed pores within the particle.

Based on the mercury porosimetry analysis, pore size distribution of particles is reported in Fig. 2.9. This method is only used to have a qualitative analysis of the pores within plant particles. It shows the three levels of porosity in hemp shiv. This is due to the structural organization of the xylem in which the conducting elements mainly consist of tracheid cells (from 5 to 50 μm) and vessels (from 50 to 300 μm). The punctuations which give the possibility for vessels to communicate can also create smaller pores. According to these results, rice husk is characterized by small pores under 0.1 μm . Almost no pores are detected from 1 to 30 μm . However, the presence of large vessels beyond 50 μm is detected. This is related to the region of vascular bundles which is common with hemp shiv.

Fig. 2.9 Pore size distribution by mercury porosimetry



2.3.3 Shape and Particle Size Distribution

Particle size distribution of plant particles is performed by means of an image analysis processing. This method has proved its worth to obtain an efficient granulometric analysis of hemp aggregates [35] whereas some studies have shown the inconsistency of mechanical sieving for particulate materials with an elongated shape [36, 37]. Unlike the use of standard sieves which ultimately separate particles according to their width, image analysis allows to represent the minor and the major axis (width and length). It is well known that the cumulative passing curve obtained by mechanical sieving is actually identical to the width distribution plotted thanks to the results of image analysis [2]. In addition, the equivalent area diameter (EQ) can be calculated as described below [29] (Eq 2.1):

$$EQ = \sqrt{\frac{4 \times \text{Area}}{\pi}} \quad (2.1)$$

Figure 2.10 shows the size distribution of defibered hemp shives coming from two different suppliers. The length of the shives from Technichanvre[®] is marginally higher than that registered for the shiv of FRD[®]. The length distribution is about 2–25 mm in both cases.

A comparison between the size distribution of hemp shiv and rice husk is done in Fig. 2.11. Critical distinctions can be drawn from this analysis. The width of rice husk ranges from 1 to 4 mm and its maximum length is 10 mm. In the case of hemp shiv, the width distribution is about the same but the length can reach up to 25–27 mm (Fig. 2.11a). As a consequence, the elongation factor (EF), defined here

Fig. 2.10 Particle size distribution of hemp shives. Cumulative granulometric distribution by image analysis (ImageJ) for *minor axis* (width), equivalent area diameter and *major axis* (length). A Area. FRD and Technichanvre are two different French suppliers

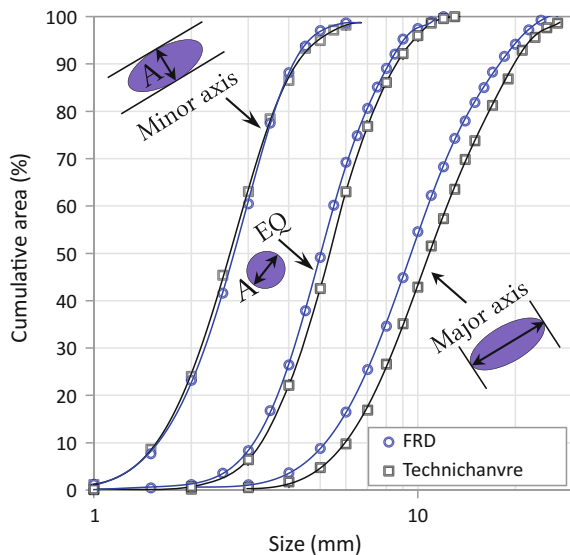
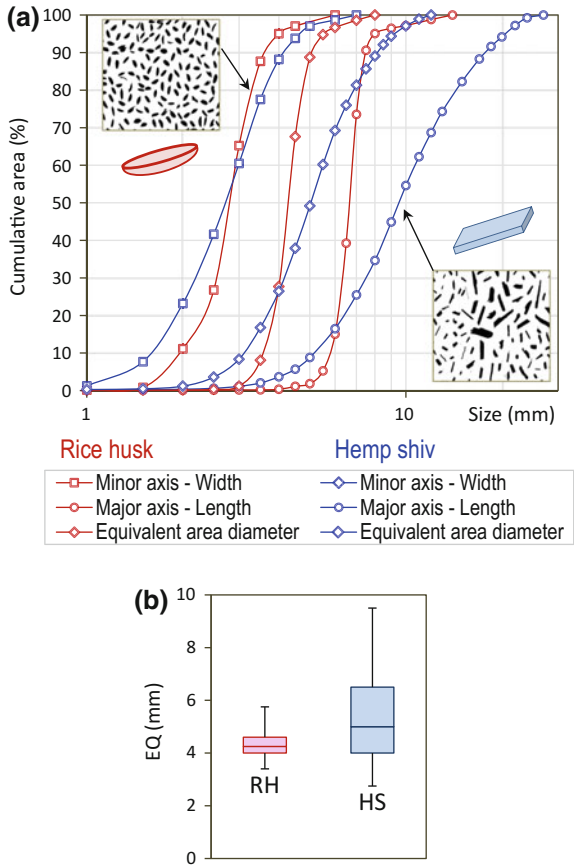


Fig. 2.11 **a** Particle size distribution of hemp shiv and rice husk **b** Statistical dispersion of the equivalent area diameter (EQ), *RH* Rice Husk,—*HS* Hemp Shiv



as the length on width ratio (L/W) is higher for hemp shiv (Table 2.3). This reflects a more spherical shape for rice husk.

The granulometric distribution of rice husk presents a very small size range in comparison to hemp shiv (Fig. 2.11a). This is the case for all the size parameters. The statistical dispersion of the equivalent area diameter represented in Fig. 2.11b highlights the major difference between rice husk particles for which the size distribution is nearly monodisperse and hemp aggregates characterized by a significant dispersion. The boxplot in Fig. 2.11b indicates that 90% of rice husks have an equivalent area diameter between 3.4 and 5.8 mm whereas it is between 2.8 and 9.5 mm for hemp shives. Furthermore, the length of rice husk is mainly distributed between 5 and 8 mm.

The small size range of rice husks is due to their origin since it is known that dimensions of rice husk particles are fully dependent on the size of rice grains, the latter showing a very low variation in a representative statistical sample. In contrast, hemp shives come from an industrial grinding process of hemp stems which

Table 2.3 Size parameters for a cumulative distribution of 50%. Median width (W_{50}), equivalent area diameter (EQ_{50}), length (L_{50}) and elongation factor (EF_{50})

Median parameters	Rice husk	Hemp shiv
W_{50} (mm)	2.8	2.7
EQ_{50} (mm)	4.3	5.2
L_{50} (mm)	6.7	10.3
EF_{50} (L_{50}/W_{50})	2.4	3.8

necessarily generates a more dispersed distribution. This more irregular shape is due to the shredding action of the size reduction machinery.

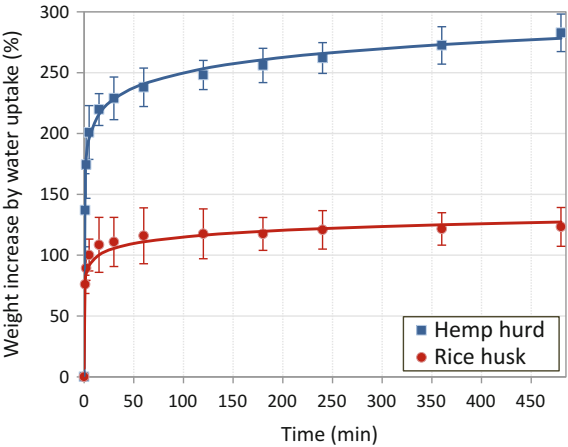
The particle size distribution provides valuable informations as it conditions the granular stacking of the plant-based concrete. Considering that the intergranular macroporosity of the concrete is linked to this granular stacking, the morphological parameters should have an influence on thermal and mechanical properties of plant-based concretes. Furthermore, a single husk is a flexible particle with a hollow semi-ellipsoidal shape and thickness lower than 100 μm (Fig. 2.6a). This geometry presents an original aspect when it is compared to the parallelepipedic shape of a hemp shiv particle (with a few millimeters thick) as regards the induced macroporosity in the concrete.

2.4 Specific Properties for Plant-Based Concretes

2.4.1 Water Absorption Capacity

Figure 2.12 reports the water absorption capacity of plant aggregates. The test consisted in immersing dried particles (48 h at 105 $^{\circ}\text{C}$) in water during 8 h and

Fig. 2.12 Mass relative water absorption of plant aggregates



following the mass uptake registered at appropriate intervals of time. Particles were put in a spherical strainer immersed in water. For each measurement, the latter was introduced into a spinner and centrifuged one minute.

For hemp shiv like rice husk, absorption kinetics is very fast during the first few minutes. The absorption rate of hemp shiv after 5 min is 200% according to Chabannes et al. [29] (Fig. 2.12). It is between 225 and 280% for other authors with different shives and various methods to test the water absorption [1, 2, 29, 38, 39]. The absorption rate of rice husk after 5 min is 100%. Beyond 5 min, a second stage takes place where the water uptake strongly decreases. During this stage, rice husks are quickly close to saturation when hemp shives keep absorbing a higher amount of water. It has been shown that hemp shiv is able to absorb nearly 4 times its dry weight after 48 h of immersion before saturation (370% [1]). Figure 2.12 shows that weight gain of immersed rice husk is about 120% after 8 h. According to Tamba et al. [40], the water absorption rate of rice husk after 20 h of immersion before saturation is 80%. Another author reports a rate of 122% [18]. No details are provided on the husk variety (e.g. parboiled or not).

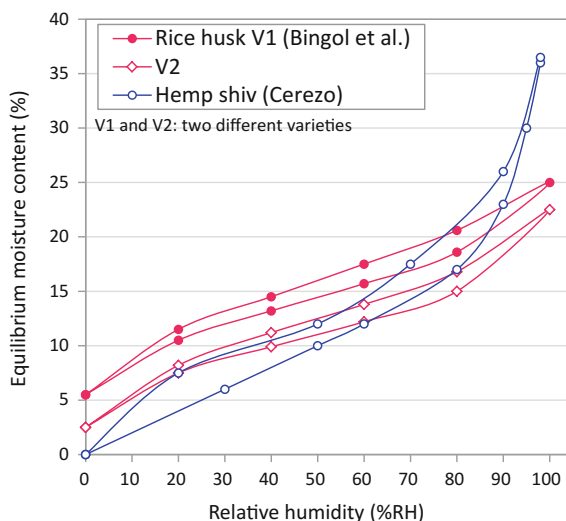
One of the difficulties encountered for designing plant-based concretes is the competition for water between the mineral binder and plant aggregates during the manufacture of the material. A lack of water for the binder due to water absorption by plant vessels can disrupt the setting of the concrete.

2.4.2 Sorption Isotherms

The use of plant aggregates with high porosity brings to consider their behavior towards water vapor. It is well known that moisture content of porous materials increases with ambient relative humidity, especially that crop by-products are hydrophilic.

Sorption isotherms of plant aggregates at 25 °C are reported in Fig. 2.13. Isotherms of type II are recognized according to the classification of Brunauer et al. [41] with a sigmoid shape (i.e. S-shape). The first part of the profiles (here for RH lower than 20%) corresponds to strongly bonded water (structural water) and monolayer water adsorbed by hydrophilic groups of particles (water is hydrogen-bonded to the hydroxyl groups of cellulose and hemicelluloses) [41]. This water would cover the external surface of the cell walls [42]. The second part between 20%RH and 70–80%RH is associated to a linear evolution of the profile. It corresponds to the continuous transition from bound to free water. The first layer of water is saturated and a multilayer adsorption takes place. The water is then present in small capillaries [41, 42]. It is seen from Fig. 2.13 that moisture content of rice husk in this range from low to mid RH is higher than that of hemp shiv. However, in the third zone (beyond 70%RH), for which water is present in the liquid state in large capillaries, the moisture content of hemp shiv begins to increase more strongly whereas that of rice husk continues to increase almost linearly up to final saturation. The equilibrium moisture content at 100%RH is 35% for hemp shiv when that of

Fig. 2.13 Sorption isotherms of rice husk [44] and hemp shiv [39]



rice husk is lower than 25%. These differences between the two kinds of particle are related to their porous structure but also to their chemical composition. Xylem vessels of hemp shiv are thick-walled tubes consisting of a polysaccharide-rich primary wall surrounding a lignified secondary cell wall. Hemp shiv is therefore highly hydrophilic and composed of large vessels as demonstrated before. This probably explains the higher sorption of water vapor in hemp shives for high RH. By contrast, the outer layer of rice husk is covered with waxes, protective pectin, silica and lignin. As a result, it is quite hydrophobic if it is compared to hemp shiv [43]. The behavior of rice husk for low RH could be explained by the presence of extremely small pores in outer layers of rice husk.

Water vapor sorption of plant aggregates has a role to play in the drying process of plant-based concretes but also towards carbonation and internal curing [45].

References

1. V. Nozahic, Vers une nouvelle démarche de conception des bétons végétaux lignocellulosiques basée sur la compréhension et l'amélioration de l'interface Liant/Végétal. Application à des granulats de chènevotte et de tige de tournesol associés à un liant ponce/chaux, Ph.D. Thesis (Clermont University, France, 2012), p. 311
2. T.T. Nguyen, Contribution à l'étude de la formulation et du procédé de fabrication d'éléments de construction en béton de chanvre, Ph.D. thesis (Bretagne-Sud University, France, 2010) p. 167
3. D. Sedan, Etude des interactions physico-chimiques aux interfaces fibres de chanvre/ciment. Influence sur les propriétés mécaniques du composite, Groupe d'étude des Matériaux Hétérogènes, Ph.D. Thesis, (Limoges University, France, 2007) p. 129
4. CETIOM, Enquête culturelle, Chanvre 2013. Available: <http://www.cetiom.fr>

5. M. Chabannes, *Formulation et étude des propriétés mécaniques d'agrobétons légers isolants à base de balles de riz et de chènevette pour l'éco-construction* (Université de Montpellier, 2015), p. 215
6. Construire en Chanvre, *Règles professionnelles d'exécution* (SEBTP. Société d'Édition du Bâtiment et des Travaux Publics, 2012)
7. E. Biénabe, A. Rival, D. Loeillet, *Développement durable et filières tropicales* (QUAE, 2016), p. 336
8. FAO, Classement mondial 2013 des pays producteurs de riz paddy, (2014) Available: <http://www.lasyntheseonline.fr>
9. W.P. Armstrong, Fruit Terminology—Part 2, (2001). Available: <http://waynesword.palomar.edu/termfr2.htm>
10. K. Ganesan, K. Rajagopal, K. Thangavel, Rice husk ash blended cement: assessment of optimal level of replacement for strength and permeability properties of concrete. *Constr. Build. Mater.* **22**(8), 1675–1683 (2008)
11. T. Serrano, M. Victoria Borrachero, J. Monzó, J. Payà, Morteros aligerados con cascarilla de arroz: diseño de mezclas evaluación de propiedades. *Dyna* **175**, 128–136 (2012)
12. R. Jauberthie, F. Rendell, S. Tamba, I. Cisse, Origin of the pozzolanic effect of rice husks. *Constr. Build. Mater.* **14**(8), 419–423 (2000)
13. V. Van, C. Röbler, D. Bui, H. Ludwig, Rice husk ash as both pozzolanic admixture and internal curing agent in ultra-high performance concrete. *Cem. Concr. Compos.* **53**, 270–278 (2014)
14. P. Chindaprasirt, S. Homwuttivong, C. Jaturapitakkul, Strength and water permeability of concrete containing palm oil fuel ash and rice husk-bark ash. *Constr. Build. Mater.* **21**(7), 1492–1499 (2007)
15. G.C. Cordeiro, R.D. Toledo Filho, L.M. Tavares, E.D.M.R. Fairbairn, S. Hempel, Influence of particle size and specific surface area on the pozzolanic activity of residual rice husk ash. *Cem. Concr. Compos.* **33**(5), 529–534 (2011)
16. W. Xu, Y.T. Lo, D. Ouyang, S.A. Memon, F. Xing, W. Wang, X. Yuan, Effect of rice husk ash fineness on porosity and hydration reaction of blended cement paste. *Constr. Build. Mater.* **89**, 90–101 (2015)
17. N. Johar, I. Ahmad, A. Dufresne, Extraction, preparation and characterization of cellulose fibres and nanocrystals from rice husk. *Ind. Crops Prod.* **37**(1), 93–99 (2012)
18. M. González De la Coteria, Morteros Ligeros de Cáscara de Arroz, in *IV Congreso Nacional de Ingeniería Civil*, 1982
19. M. Ibrahim Nasr Morsi, Properties of rice straw cementitious composite, PhD Thesis (Darmstadt University, Germany, 2011) p. 147
20. D.M. Alonso, S.G. Wettstein, J.A. Dumesic, Bimetallic catalysts for upgrading of biomass to fuels and chemicals. *Chem. Soc. Rev.* **41**(24), 8075–8098 (2012)
21. Y. Diquélou, E. Gourlay, L. Arnaud, B. Kurek, Impact of hemp shiv on cement setting and hardening: influence of the extracted components from the aggregates and study of the interfaces with the inorganic matrix. *Cem. Concr. Compos.* **55**, 112–121 (2014)
22. C. Garcia-Jaldon, D. Dupeyre, M.R. Vignon, Fibres from semi-retted hemp bundles by steam explosion treatment. *Biomass Bioenerg.* **14**(3), 251–260 (1998)
23. K.G. Mansaray, A.E. Ghaly, Thermal degradation of rice husks in an oxygen atmosphere. *Energy Sources* **21**(5), 453–466 (1999)
24. T.P.T. Tran, J.-C. Bénézet, A. Bergeret, Rice and Einkorn wheat husks reinforced poly(lactic acid) (PLA) biocomposites: effects of alkaline and silane surface treatments of husks. *Ind. Crops Prod.* **58**, 111–124 (2014)
25. M. Chabannes, E. Garcia-Diaz, L. Clerc, J.C. Bénézet, Effect of curing conditions and Ca (OH)₂-treated aggregates on mechanical properties of rice husk and hemp concretes using a lime-based binder. *Constr. Build. Mater.* **102**, 821–833 (2016)
26. P. Glé, Acoustique des Matériaux du Bâtiment à base de Fibres et Particules Végétales. Outils de Caractérisation, Modélisation et Optimisation, PhD Thesis (École Nationale des Travaux Publics de l'État, France, 2013) p. 127

27. B.-D. Park, S.G. Wi, K.H. Lee, A.P. Singh, T.-H. Yoon, Y.S. Kim, Characterization of anatomical features and silica distribution in rice husk using microscopic and micro-analytical techniques. *Biomass Bioenerg.* **25**(3), 319–327 (2003)
28. A. Kaupp, *Gasification of rice hulls: theory and Praxis* (Vieweg + Teubner Verlag, Wiesbaden, 1984)
29. M. Chabannes, J.-C. Bénézet, L. Clerc, E. Garcia-Diaz, Use of raw rice husk as natural aggregate in a lightweight insulating concrete: an innovative application. *Constr. Build. Mater.* **70**, 428–438 (2014)
30. J. Salas and J. Veras Castro, Materiales de construcción con propiedades aislantes a base de cascara de arroz. *Inf. la Constr.* **37**(372), 53–64 (2012)
31. R. Rowell, Moisture properties, in *Handbook of wood chemistry and wood composites* (CRC Press, Boca Raton, 2005), p. 21
32. F. Collet, M. Bart, L. Serres, J. Miriel, Porous structure and water vapour sorption of hemp-based materials. *Constr. Build. Mater.* **22**(6), 1271–1280 (2008)
33. A. Prada, C.E. Cortés, La descomposición térmica de la cascarilla de arroz: una alternativa de aprovechamiento integral. *Rev. ORINOQUIA* **14**(1), 155–170 (2010)
34. A. Kaupp, J. Goss, Technical and economical problems in the gasification of rice hulls. Physical and chemical properties. *Energy Agric.* **1**, 201–234 (1983)
35. V. Nozahic, S. Amziane, G. Torrent, K. Saïdi, H. De Baynast, Design of green concrete made of plant-derived aggregates and a pumice–lime binder. *Cem. Concr. Compos.* **34**(2), 231–241 (2012)
36. V. Picandet, P. Tronet, C. Baley, *Caractérisation granulométrique des chènevottes*, in *30e Rencontres AUGC-IBPSA* (Chambéry, France, 2012)
37. C. Igathinathane, L.O. Pordesimo, E.P. Columbus, W.D. Batchelor, S. Sokhansanj, Sieveless particle size distribution analysis of particulate materials through computer vision. *Comput. Electron. Agric.* **66**(2), 147–158 (2009)
38. L. Arnaud, E. Gourlay, Experimental study of parameters influencing mechanical properties of hemp concretes. *Constr. Build. Mater.* **28**(1), 50–56 (2012)
39. V. Cerezo, Propriétés mécaniques, thermiques et acoustiques d'un matériau à base de particules végétales : approche expérimentale et modélisation théorique, PhD Thesis (École Nationale des Travaux Publics de l'État, Lyon, France 2005), p. 243
40. S. Tamba, I. Cisse, F. Rendell, R. Jauberthie, *Rice husk in lightweight mortars*, in *Second international symposium on structural lightweight aggregate concrete* (Kristiansand, Norway, 2000), pp. 117–124
41. R.D. Andrade, R. Lemus, C. Pérez, Models of sorption isotherms for food. *Vitae* **18**, 325–334 (2011)
42. M.V. Bastias, A. Cloutier, Evaluation of wood sorption models for high temperatures. *Maderas Ciencias y Tecnol.* **7**(3), 145–158 (2005)
43. A. Bazargan, T. Gebreegziabher, C.-W. Hui, G. McKay, The effect of alkali treatment on rice husk moisture content and drying kinetics. *Biomass Bioenerg.* **70**, 468–475 (2014)
44. G. Bingol, B. Prakash, Z. Pan, Dynamic vapor sorption isotherms of medium grain rice varieties. *LWT—Food Sci. Technol.* **48**(2), 156–163 (2012)
45. P. Lura, M. Wyrzykowski, C. Tang, E. Lehmann, Internal curing with lightweight aggregate produced from biomass-derived waste. *Cem. Concr. Res.* **59**, 24–33 (2014)

Lime Hemp and Rice Husk-Based Concretes for Building
Envelopes

Chabannes, M.; Garcia-Diaz, E.; Clerc, L.; Bénézet, J.-C.;
Becquart, F.

2018, VIII, 104 p. 68 illus., Softcover

ISBN: 978-3-319-67659-3